Fabrication of multilayer organic solar cells through a stamping technique†

Jen-Hsien Huang,[a] Zhong-Yo Ho,[b] Tsung-Hsien Kuo,[a] Dhananjay Kekuda,[c] Chih-Wei Chu*[cd] and Kuo-Chuan Ho*[ab]

Received 24th February 2009, Accepted 24th April 2009
First published as an Advance Article on the web 7th May 2009
DOI: 10.1039/b903765a

In this article, we demonstrate a simple and reliable stamping technique for fabricating multi-layer solar cells. A poly(di-methyl-silane) (PDMS) stamp is used for transferring the active layers onto the substrate. An intermediate solvent treatment is introduced to temporarily modify the PDMS surface; therefore, the polymer film can be uniformly formed on top of the PDMS surface. This method is involves non-contaminative and non-invasive processes, therefore it can avoid possible degradation or contamination of the polymer film and the PDMS stamp can be reused. Devices realized through this stamping technique both by direct and inverted structures exhibited power conversion efficiencies of 3.2 and 2.83% respectively.

1. Introduction

Organic semiconductors (OSs) have received a great deal of attention from both academic and industrial laboratories because of their processing advantages as well as their mechanical properties. Since these OSs can be easily solution processed, they are considered to be a promising candidate for high throughput, low-cost and large area fabrication of optoelectronics, such as light emitting diodes (LEDs),[1,2] thin film transistors (TFTs),[3,4] and solar cells (SCs).[5,6] Considerable progress has been made in designing solution-processed organic semiconductors; however, the performance of the devices is somehow restricted by their relatively poor carrier transfer properties and large energy bandgaps, which result in poor performance compared to most of their inorganic counterparts. While the inherent material properties of these OSs are important in achieving the desired output of the device, the device structure is another primary factor for achieving efficient devices. For example, time-consuming thermal vacuum deposition for small molecules could fulfil the multilayer and tandem structure *via* layer by layer deposition.[8,9] Alternatively, in order to reduce the time scale of the manufacturing process, solution processing of the active layer components could be utilized. However, dissolution of the initial layer by the subsequent layers during spin coating acts as a barrier to the realization of multilayer spin coating films. Different approaches have been employed by earlier researchers to overcome such issues which include utilization of cross-linking polymers,[10,11] use of different solvents for subsequent layers[12] or through insertion of intermediate buffer layers to protect the preceding layers.[13,14] The drawback in the former case is that the performance of polymers is decreased after the cross-linking process. A disadvantage of the latter case is that only a limited combination of materials and solvents can be chosen. Therefore, besides those recent advances, there is a great demand for fabricating innovative multi-layer structures through a simple and reliable technique which can be utilized for both single and multilayer films.

Recently, a relatively new technique called the PDMS lamination process was used in the area of organic electronics for connecting metal to organics,[15,16] organics to metal,[16,17] and organics to organics.[18–21] Proceeding further, Kim and co-workers modified the PDMS lamination process for transfer printing and fabricated bi-layer polymer LEDs and SCs.[22] They used a sacrificial layer cast on silicon wafer, allowing the PDMS to attach to the solid objects on the silicon wafer modified with sacrificial layer. Although this method prevents the dissolution problem, this method is too complicated and the residual of sacrificial layer will contaminate the interface between two organic layers, resulting in a decrease in device performance. In order to overcome these drawbacks, Bradley and co-workers modified the surface of PDMS by plasma treatment which made the polymer films able to cast on the PDMS directly.[23] However, the destructive physical treatment procedure not only complicates the whole process but also causes serious damage to the surface structure of PDMS due to the high power plasma treatment. This influences the morphology of the transferred polymer films leading to poor solar cell performance. In this Communication, we modified the printing method by increasing the affinity of PDMS for organic solvents *via* non-destructive solvent treatment. This stamping method eliminates the necessity of any plasma treatment and any possible damages on the PDMS surface and would give full control over the chemical composition and film thickness of each layer. The multilayer polymer structure also demonstrates use in photovoltaic applications.

2. Experimental

PDMS stamps were synthesized from an oligomer (Silgard 184A) and a curing agent, which was mixed in the ratio of 10:1 by volume. After the mixing, it was poured onto silicon wafer to achieve a smooth surface stamp and then placed in vacuum for one hour to remove the air bubbles. When all the bubbles were removed the mould with the PDMS was placed in the oven for curing for 3–4 hours at 70 °C. Afterwards the cured PDMS was removed from the mould and cut into the appropriate dimensions. The bulk heterojunction (BHJ) SCs in this study consist of a layer of

[a]*Department of Chemical Engineering, National Taiwan University, Taipei, Taiwan 10617. E-mail: kcho@ntu.edu.tw*
[b]*Institute of Polymer Science and Engineering, National Taiwan University, Taipei, Taiwan 10617*
[c]*Research Center for Applied Sciences, Academia Sinica, Taipei, Taiwan 11529. E-mail: gchu@gate.sinica.edu.tw*
[d]*Department of Photonics, National Chao-Tung University, Hsinchu 30010, Taiwan*
† Electronic supplementary information (ESI) available: Experimental details. See DOI: 10.1039/b903765a

poly(3-hexylthiophene):[6,6]-phenyl C61-butyric acid methyl ester (P3HT:PCBM) blend thin film sandwiched between transparent anode indium tin oxide (ITO) and metal cathode. Before device fabrication, the ITO glasses (1.5 × 1.5 cm^2) were ultrasonically cleaned in detergent, de-ionized water, acetone and isopropyl alcohol before the deposition. After routine solvent cleaning, the substrates were treated with UV ozone for 15 min. Then a modified ITO surface was obtained by spin-coating a layer of poly(ethylene dioxythiophene): polystyrenesulfonate (PEDOT:PSS) (~30 nm). Subsequently, the active layer of P3HT:PCBM (1:1 w/w) was transferred from the PDMS stamp onto the PEDOT:PSS modified ITO surface. The whole transfer process was performed in a nitrogen-filled glove box. Finally, 30 and 100 nm thick calcium and aluminum were thermally evaporated under vacuum at a pressure below 6×10^{-6} Torr thorough a shadow mask. The active area of the device was 0.12 cm^2. For the inverted solar cell based on P3HT and PCBM, a caesium carbonate (Cs_2CO_3) electron injection layer was cast on the ITO substrate which was prepared according to the previous work.[24] Then, a PCBM layer was spin cast from chloroform subsequently the P3HT was transferred from PDMS stamp. The thicknesses of PCBM and P3HT were controlled at 40 and 100 nm cast from chloroform. Upon completion of the transfer process, the target sample (ITO/Cs_2CO_3/PCBM/P3HT) was transferred to a vacuum chamber to deposit the anode electrodes for the SCs, which consist of V_2O_5 (10 nm) and Al (70 nm).

The solar cell testing was done inside a glove box under simulated AM 1.5 G irradiation (100 W/cm^2) using a Xenon lamp based solar simulator (Thermal Oriel 1000 W). The absorption and photoluminescence (PL) spectra were obtained from Jasco-V-670 UV-visible spectrophotometer and Hitachi F-4500, respectively. Images of the surface morphorlogy and cross sections of thin films were obtained using atomic force microscopy (AFM, Digital instrument).

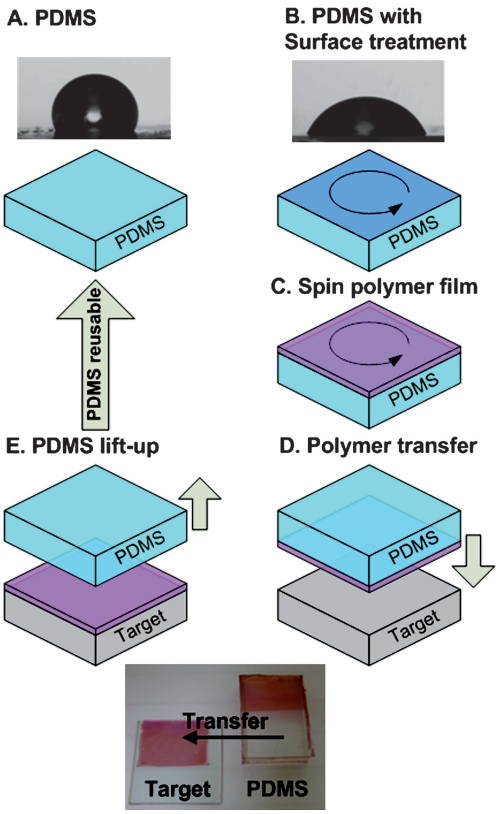

Fig. 1 A schematic of the procedure for the thin film conveying technique by PDMS stamps. (a) PDMS stamps prepared on silicon wafer, (b) the PDMS stamp was treated with organic solvents *via* spin coating, (c) the polymer film was spun directly on the PDMS stamp, (d) the films spun on PDMS surface were transferred to the target substrate (e) after transferring, the PDMS stamp was lifted up which can be reused.

3. Results and discussion

The transferring scheme used here is illustrated in Fig. 1. Initially, the surface of PDMS stamps was treated with organic solvents depending on the solvent used for dissolving the polymers (Fig. 1b). It is also critical to maintain homogeneity of the polymer film with residual solvent vapor around PDMS surface. The residual solvent vapor can change the surface energy of PDMS with carefully controlled the spin rate which decreases the chloroform contact angle significantly as shown in Fig. 1a and b. Consequently, the polymer film can be directly spun onto the PDMS surface after solvent treatment (Fig. 1c). The stamping process was then carried out by attaching the polymer film coated on PDMS stamp onto the target surface under thermal and physical driving forces (Fig. 1d). It is anticipated that near the glass transition temperature, the transfer of films from the PDMS to the target surface takes place effectively and hence the stamping process was carried out at 120 °C. After transferring the polymer film, the PDMS stamps could be reused for next batch of film transfer process (Fig. 1a). The photograph in the bottom of Fig. 1 reveals the image of PDMS cast with P3HT after the stamping process.

In general, the stamping process depends on the external force applied and the temperature at which the process takes place. The sticking coefficient between the polymer film, the target substrate, and PDMS surface determines the magnitude of force required for the stamping process. In order to prevent shear stress, the external force applied during the stamping process was kept as low as 4.35×10^4 Pa. The stamping temperature is the other important issue in the process which provides a driving force for polymer transfer. Around the glass transition temperature of polymer, it is anticipated that there would be fewer voids at the interface than for a room temperature stamping process. Since the stamping process involves the simultaneous application of external force and heat treatment, there is a possibility of mechanical damage of the active layer as well as PDMS stamps. In order to observe the variation in morphology of the PDMS before and after transferring process, atomic force microscopy (AFM) was used. As can be seen from the AFM images in Fig. 2, it is clear that the P3HT film spun on PDMS surface reveals a chain-like feature which is assigned to the stack of P3HT chains with a root mean square roughness (RMS) of 7.8 nm (Fig. 2a). In contrast, the AFM image of the PDMS shows a much smoother morphology with a RMS of 1.1 nm (Fig. 2b) after the stamping process. The smooth morphology is expected because PDMS stamps were moulded on Si wafer and hence follows the surface roughness of silicon wafer, which is fairly smooth. Hence, from the variation of surface roughness, it indicates that the polymer film can be completely transferred to the target surface without damage.

In order to further examine the feasibility of the stamping process for the fabrication of bilayer and multilayer devices, the transferring a polymer layer onto another polymer layer is important and hence

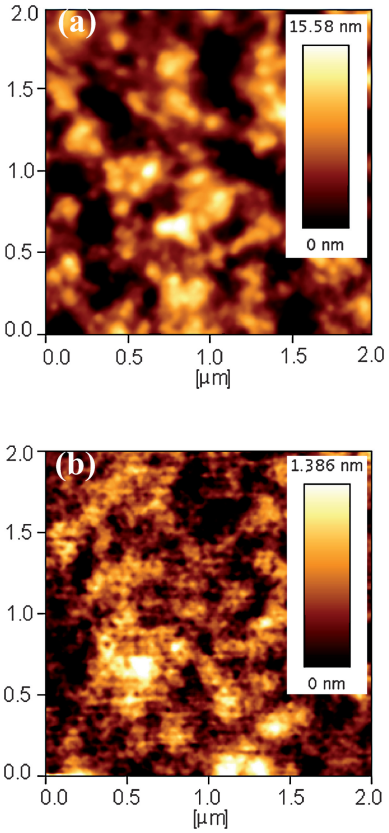

Fig. 2 AFM images of (a) the P3HT cast from chloroform onto the PDMS (b) the PDMS surface morphology after the completion of transfer process.

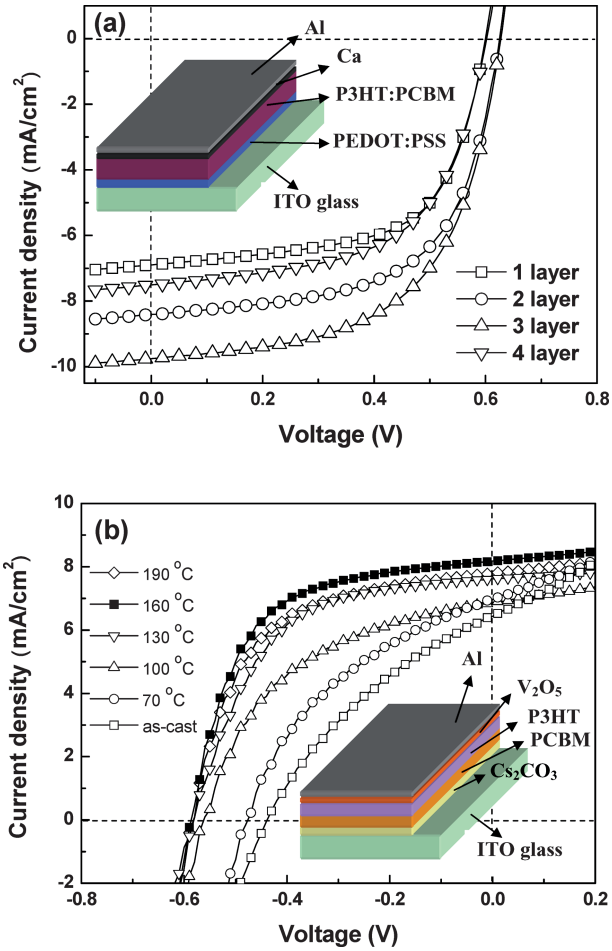

Fig. 3 The cell performance tested under AM 1.5 G (100 mW cm^{-2}) for (a) the BHJ SCs with different numbers of active layer based on P3HT:PCBM (1:1 in wt%) fabricated by PDMS transfer process. (b) The inverted bi-layer structure at various annealing temperatures.

was investigated by fabricating the multilayer BHJ SCs. The P3HT:PCBM (1:1) layers were cast from chloroform and the thickness was controlled at 100 nm. The total number of layers was varied from 1 to 4 and its dependence on the device performance is monitored. In order to improve the interface between the different active layers, we annealed the samples at 130 °C after transferring each active layer. The duration of annealing was 5 min. Finally, a 30 and 100 nm thick Ca and Al was thermally evaporated. The device structure is shown in Fig. 3a. The short circuit current (J_{SC}) gradually increased from 6.89 mA/cm^2 for a single layer system (100 nm) to as high as 9.74 mA/cm^2 for a three layered systems (300 nm), and finally reduced to 7.52 mA/cm^2 (400 nm) as shown in Fig. 3a. The increase of J_{SC} can be explained by the larger fraction of solar light absorbed by those devices with thicker active layer. Although the absorbance can be increased further by the increase of the active layer thickness, the J_{SC} decreases to 7.52 mA/cm^2 for the devices with four active layers. The decrease of J_{SC} is due to the poor transport for photogenerated charges leading to a serious charge recombination. The triple layered devices exhibited a cell performance with an efficiency of ~3.55%. It is worthy to mention that the fill factor (FF) of devices with 1 layer and 3 layers are 62.0 and 62.7% and the corresponding open circuit voltage (V_{OC}) are 0.60 and 0.61 V, respectively. The similar FF and V_{OC} indicate that the quality interfaces can be formed between each layer through stamping process. Moreover, the tandem polymer SCs and polymer LEDs can also be achieved through this stamping process by incorporating the connecting layers, such as silver nanoparticles.[25]

In order to further demonstrate the surface modified stamping process, we have also fabricated inverted bi-layer SCs. The schematic of the devices is shown in inset of Fig. 3b. Fig. 3b shows the performance of the inverted cells under various annealing temperatures. For the device without thermal annealing after the transferring process, the power conversion efficiency (PCE) is 0.97%. This can be understood from the AFM image in Fig. 2a. The transferred P3HT film typically has a fairly rough surface that caused some portion of P3HT surface not to touch the underlying PCBM. In that case, voids will be developed between the P3HT and PCBM thin films, resulting in poor device performance. However, this problem can be easily resolved by the annealing process. As the annealing temperature increases from room temperature to 160 °C, all of device characteristics, such as V_{OC}, J_{SC}, and FF, are improved. The devices can be activated leading to an increase of PCE from 0.97 to 2.83%. The optimal annealing temperature is determined within the range of 160–190 °C, which is higher than the glass transition temperature of P3HT.[26] The enhancement is attributed to reorganize the polymer and therefore the voids are reduced and more interfaces can be provided for exciton dissociation. The devices shown better performance than most of small molecule bi-layer SCs made *via* thermal evaporation process[27–29] and also shown better performance

Table 1 A summary of the BHJ and bi-layer cell performance of parameters, indicating J_{SC}, V_{OC}, FF and PCE as a function of the number of active layer and annealing temperature

Sample	J_{SC}/mA cm^{-2}	V_{OC}/V	FF (%)	PCE (%)
BHJ device				
1 layer	6.90	0.60	62.0	2.56
2 layer	8.41	0.61	62.1	3.18
3 layer	9.75	0.61	62.7	3.55
4 layer	7.51	0.60	58.6	2.64
Bi-layer device				
As-cast	6.43	0.44	34.2	0.97
70 °C	6.96	0.48	39.8	1.33
100 °C	6.87	0.56	48.1	1.85
130 °C	7.62	0.58	55.9	2.47
160 °C	8.18	0.58	59.6	2.83
190 °C	7.79	0.58	57.7	2.61

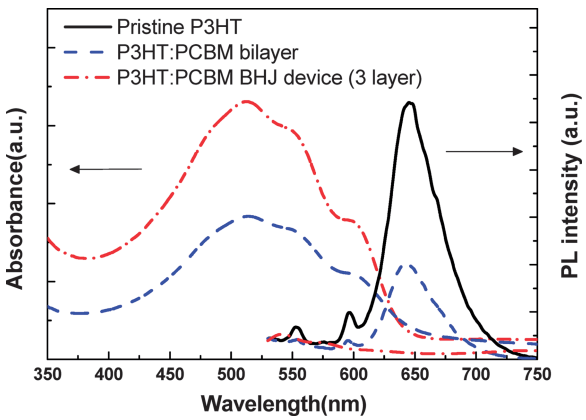

Fig. 4 Absorbance and PL quenching results for bi-layer and BHJ SCs fabricated from PDMS stamping process.

compared with devices made by other polymer transfer techniques.[22,23] However, the efficiency is slight lower compared to P3HT:PCBM based BHJ SCs. Although bi-layer structures can have higher hole and electron collection efficiency, it provides fewer interfaces for exciton dissociation compared to BHJ. All the performance parameters for the BHJ and bi-layer devices, namely J_{SC}, V_{OC}, FF and PCE as a function of the number of active layer and annealing temperatures are summarized in Table 1. From the photoluminescence (PL) spectra shown in Fig. 4, it can be seen that excitons is not be fully quenched in bi-layer structure, but in BHJ structure the quenching is more efficient. Furthermore the absorption of bi-layer SCs is also smaller than the one of BHJ SCs. The optimization of the P3HT and PCBM thickness can be expected to improve the quenched capability and absorption of P3HT:PCBM bilyaer SCs, resulting in further improving the device efficiency.

4. Conclusion

In summary, the polymer–polymer and polymer–small molecule interfaces were successfully demonstrated thorough a PDMS stamping technique without destroying the preceding layers. The electrical and optical investigations infer that this stamping method can easily fabricate the multilayer organic optoelectronics. Combining this with careful design of the device structure and matching materials with suitable properties, it is anticipated that the PDMS transfer technique allows us to fabricate tandem or cascade polymer LEDs and polymer SCs with better performance, which is under our investigation.

Acknowledgements

The authors are grateful to the National Science Council (NSC), Taiwan, (NSC 96-2120-M-002-016 and NSC 96-2221-E-001-017-MY2) and Academia Sinica research program on Nanoscience and Nanotechnology for financial support.

Notes and references

1 R. H. Friend, R. W. Gymer, A. B. Holmes, J. H. Burroughes, R. N. Marks, C. Taliani, D. D. C. Bradley, D. A. Dos Santos, J. L. Bredas, M. Logdlund and W. R. Salaneck, *Nature*, 1990, **397**, 121.
2 P. K. H. Ho, J.-S. Kim, J. H. Burroughes, H. Becker, S. F. Li, T. M. Brown, F. Cacialli and R. H. Friend, *Nature*, 2000, **404**, 481.
3 L. L. Chua, J. Zaumseil, J.-F. Chang, E. C. W. Ou, P. K. H. Ho, H. Sirringhaus and R. H. Friend, *Nature*, 2005, **434**, 194.
4 H. Sirringhaus, P. J. Brown, R. H. Friend, M. M. Nielsen, K. Bechgaard, B. M. W. Langeveldvoss, A. J. H. Spiering, R. A. J. Janssen, E. W. Meijer, P. Herwig and D. M. Deleeuw, *Nature*, 1999, **401**, 685.
5 J. J. M. Halls, C. A. Walsh, N. C. Greenham, E. A. Marseglia, R. H. Friend, S. C. Moratti and A. B. Holmes, *Nature*, 1995, **376**, 498.
6 G. Li, V. Shrotriya, J. Huang, Y. Yao, T. Moriarty, K. Emery and Y. Yang, *Nat. Mater.*, 2005, **4**, 864.
7 G. Yu, J. Gao, J. C. Hummelen, F. Wudl and A. J. Heeger, *Science*, 1995, **270**, 1789.
8 C. W. Tang, *Appl. Phys. Lett.*, 1986, **48**, 183.
9 C. W. Tang and S. A. Vanslyke, *Appl. Phys. Lett.*, 1987, **51**, 913.
10 H. Yan, B. J. Scott, Q. L. Huang and T. J. Marks, *Adv. Mater.*, 2004, **16**, 1948.
11 Z. Liang and O. M. Cabarcos, *Adv. Mater.*, 2004, **16**, 823.
12 W. Ma, P. K. Iyer, X. Gong, B. Liu, D. Moses, G. C. Bazan and A. J. Heeger, *Adv. Mater.*, 2005, **17**, 274.
13 S. R. Tseng, S. C. Lin, H. F. Meng, H. H. Liao, C. H. Ye, H. C. Lai and S. F. Horng, *Appl. Phys. Lett.*, 2006, **88**, 163501.
14 S. R. Tseng, H. F. Meng, C. H. Ye, H. C. Lai, S. F. Horng, H. H. Liao, C. S. Hu and L. C. Lin, *Synth. Metal.*, 2008, **158**, 130.
15 Y. L. Loo, R. L. Willett, K. W. Baldwin and J. A. Rogers, *Appl. Phys. Lett.*, 2002, **81**, 562.
16 Y. L. Loo, R. L. Willett, K. W. Baldwin and J. A. Rogers, *J. Am. Chem. Soc.*, 2002, **124**, 7654.
17 M. L. Chabinyc, A. Salleo, Y. Wu, P. Liu, B. S. Ong, M. Heeney and I. McCulloch, *J. Am. Chem. Soc.*, 2004, **126**, 13928.
18 M. Granstrom, K. Petritsch, A. C. Arias, A. Lux, M. R. Andersson and R. H. Friend, *Nature*, 1998, **395**, 257.
19 T. F. Guo, S. Pyo, S. C. Chang and Y. Yang, *Adv. Funct. Mater.*, 2001, **11**, 339.
20 J. Huang, G. Li and Y. Yang, *Adv. Mater.*, 2008, **20**, 415.
21 H. Kim, B. Yoon, J. Sung, D. G. Choi and C. Park, *J. Mater. Chem.*, 2008, **18**, 3489.
22 K. H. Yim, Z. J. Zheng, Z. Liang, R. H. Friend, W. T. S. Huck and J. S. Kim, *Adv. Funct. Mater.*, 2008, **18**, 1012.
23 L. C. Chen, P. Degenaar and D. D. C. Bradley, *Adv. Mater.*, 2008, **20**, 1679.
24 H. H. Liao, L. M. Chen, Z. Xu, G. Li and Y. Yang, *Appl. Phys. Lett.*, 2008, **92**, 173303.
25 A. Yakimov and S. R. Forrest, *Appl. Phys. Lett.*, 2002, **80**, 1667.
26 K. Youngkyoo, S. A. Choulis, J. Nelson and D. D. C. Bradley, *Appl. Phys. Lett.*, 2005, **86**, 063502.
27 C. W. Chu, Y. Shao, V. Shrotriya and Y. Yang, *Appl. Phys. Lett.*, 2005, **86**, 243506.
28 R. F. Salzman, J. Xue, B. P. Rand, A. Alexander, M. E. Thompson and S. R. Forrest, *Org. Electron.*, 2005, **6**, 242.
29 C. W. Chu, V. Shrotriya, G. Li and Y. Yang, *Appl. Phys. Lett.*, 2006, **88**, 153504.

